CEA/SACLAY
DSM

SERVICE DE PHYSIQUE NUCLÉAIRE

DAPNIA/SPhN-96-33

10/1996

Radiative corrections to Virtual Compton Scattering

D. Marchand, D. Lhuillier,
M. Vanderhaeghen and J. Van de Wiele

DAPNIA

Département d'Astrophysique, de Physique des Particules, de Physique Nucléaire et de l'Instrumentation Associée
CEA/Saclay F-91191 Gif-sur-Yvette Cédex

Couverture Sylvie Cabrit et Marc Sauvage

Le DAPNIA (Département d'Astrophysique, de physique des Particules, de physique Nucléaire et de l'Instrumentation Associée) regroupe les activités du Service d'Astrophysique (SAp), du Département de Physique des Particules Elémentaires (DPhPE) et du Département de Physique Nucléaire (DPhN).

Adresse : DAPNIA, Batiment 141
CEA Saclay
F - 91191 Gif s.u. Yvette Cedex

RADIATIVE CORRECTIONS TO VIRTUAL COMPTON SCATTERING

Dominique MARCHAND, David LHUILLIER, Marc VANDERHAEGHEN
CEA/DSM/DAPNIA/SPhN, CE Saclay,
91191 Gif-Sur-Yvette Cedex, France

Jacques VAN DE WIELE
IN2P3, IPN d'Orsay, 91406 Orsay Cedex, France

Radiative corrections to virtual Compton scattering are calculated for the first time at the first higher order in α. We use the dimensional regularization scheme to treat both Ultra-Violet and Infra-Red divergences. After the compensation of divergences, the expression of the correction contains analytical terms and a numerical term which has to be computed. For a scattered photon of centre of mass energy q'=45MeV, a preliminary result of the comparison between theory and experimental data is presented taking into account only analytical terms.

Two types of radiative corrections have to be considered: the external radiative corrections and the internal radiative corrections. External radiative corrections take into account the interaction of particles with the target medium whereas internal radiative corrections, which will be considered in detail in the following, originate from the p(e,e'p')γ reaction itself.

Virtual Compton scattering is accessible through photon electroproduction reaction p(e,e'p')γ. As the cross section of this process is proportionnal to α^3 (α: fine structure constant), all the diagrams which contribute to the order α^4 have to be taken into account for the internal radiative corrections. The latter have two components: one coming from the emission of a real photon, called real radiative correction, and the other one coming from processes where a virtual photon is emitted and re-absorbed, called virtual radiative corrections. We will then apply our results to data which were taken at the Mainz Microtron MAMI (reference [1]).

1 - External radiative corrections

These corrections take into account the Bremsstrahlung radiation emitted by incoming and outgoing electrons, in the target medium. The experiment performed in Mainz uses a 4.8cm extended liquid H_2 target. The target walls are made of a 9 μm Havar film.

External radiative corrections have been taken into account by L. Van Hoorebeke [2] at the level of the solid angle determination.

2 - Internal radiative corrections

We have to distinguish the virtual radiative corrections from the real ones. In order to define the vocabulary used for the calculation of radiative correction, I will first take the example of the elastic scattering.

2.1 Virtual radiative corrections

These corrections are of three types which are shown on figure 1 and correspond to the emission and the re-absorption of virtual photons.

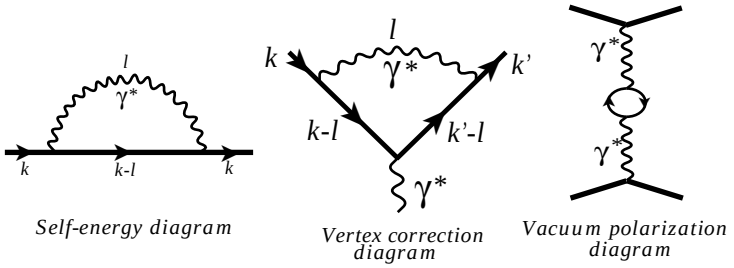

Figure 1: virtual radiative corrections.

In the calculation of the virtual radiative corrections, defined by the graphs above, one encounters the well known difficulty of U.V. divergences: the integrals over ℓ (the exchanged four-momentum) diverge with high values of ℓ and require renormalizations. In self-energy and vertex correction diagrams, another type of divergence appears in Feynman integrals: integrals diverge as ℓ tends to zero. This latter divergence is thus called I.R. divergence. The treatement of divergences is described in section 2.3

2.2 ***Real radiative corrections***

We have to consider also additional emission of real photons radiated mainly by electrons.

In the calculation of the real radiative corrections , one has to perform an integral over the space phase of the real photon of momentum $\vec{\ell}$ which presents an I.R. divergence when $\vec{\ell}$ tends to zero. In others words that means that the probability for an electron to radiate photons of very small energy is infinite.

We will see in the following section 2.3 how I.R divergences, coming on the one hand in virtual radiative corrections and on the other hand in real radiative corrections, will be finally compensated exactly when calculating cross sections. Extra real photon emission can be treated separately from others processes because the final state is different. Besides, this correction is dependent on the experimental energy cut.

2.3 ***Divergences treatement***

2.3.1 *Ultra-Violet divergences*

Self-energy integrals are U.V. linearly divergent. After a "mass" renormalization integrals become U.V. logarithmically divergent just as integrals coming from vertex diagram. These logarithmic divergences are compensated in the total sum of vertex and self-energy diagrams. This compensation is a consequence of the Ward identity which itself comes from the gauge invariance of the theory.

It subsists the U.V. divergence appearing in the vacuum polarization graph. This divergence is eliminated by performing a "charge" renormalization.

2.3.2 *Infra-Red divergences*

Logarithmic Infra-Red divergences appear in the self-energy diagram, in the vertex diagram and in the real photons emission process. By adding the cross section for the soft photon emission process and the cross section for the soft virtual photon contributions to the original process, the I.R. divergences cancel. The "miracle" of the I.R. compensation has been demonstrated within the framework of QED in 1937 [4]. This implies that all the I.R. divergent terms are cancelled in the compensation but we have to extract all the finite terms which contribute to the calculation.

For elastic scattering, one can write its scattering amplitude as:

$$A = A_0 + A_1 + A_2 ... \tag{1}$$

where A_0 is of the order α (lowest order), A_1 of order α^2 (first higher order). If we call B, of order $\alpha^{\frac{3}{2}}$ the amplitude for single real photon emission and neglecting terms which contribution to the cross section is of order higher than α^3, we can approximate the measured cross section as follows:

$$\sigma_{measured} = |A_0|^2 + 2.\mathcal{R}e(A_0.A_1) + |B|^2 = |A_0|^2(1 + \delta_v + \delta_r) \qquad (2)$$

where δ_v is for virtual radiative correction and δ_r for real radiative correction. The final goal is to access to $|A_0|^2$ from the measured cross section.

The figure 2 summarizes the divergences elimination process.

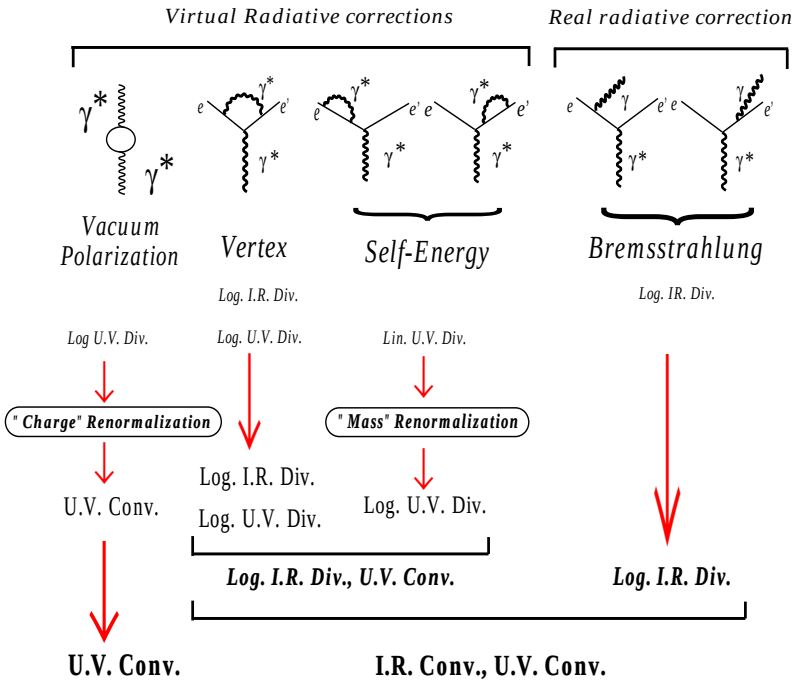

Figure 2: Summarize of divergences elimination process for elastic scattering.

2.3.3 *Dimensional regularization and Feynman parametrization*

Among all the different techniques existing to treat divergences in QED, we adopt the method of dimensional regularization [5,6].

Dimensional regularization consists in calculating integrals over a **D**-dimension space, $\mathbf{D} = 4 - \epsilon$, instead of the usual 4-dimension space.

We will see in the example below the behaviour of the integral **I** (Eq. 3) according to **D** value. (This integral corresponds to the vertex correction graph for elastic scattering.)

$$I = \frac{\epsilon^3}{(2\pi)^{\mathbf{D}}} \int d^{\mathbf{D}}\ell \frac{\gamma_\nu(\not{k}' - \not{\ell} + m)\gamma_\mu(\not{k} - \not{\ell} + m)\gamma^\nu}{(\ell^2 + i\epsilon)(\ell^2 - 2\ell.k' + i\epsilon)(\ell^2 - 2\ell.k + i\epsilon)} \tag{3}$$

- For $\ell \to 0$, $\mathbf{D} = 4$: $I \propto \int \frac{d^4\ell}{\ell^2(-2\ell.k')(-2\ell.k)} = \int \frac{d^4\ell}{\ell^4}$: Infra-Red Divergence. If $\mathbf{D} > 4$, $\mathbf{I}(D)$ converge.

- For $\ell \to \infty$, $\mathbf{D} = 4$: $I \propto \int \frac{d^4\ell(\not{\ell}\not{\ell})}{\ell^2\ell^2\ell^2} = \int \frac{d^4\ell}{\ell^4}$: Ultra-Violet Divergence. If $\mathbf{D} < 4$, $\mathbf{I}(D)$ converge.

In **D**-dimension space, integrals are calculable and divergent terms appear in pole form of $\frac{1}{\epsilon_{IR}}$ or $\frac{1}{\epsilon_{UV}}$ ($\epsilon_{UV} > 0$ when $D < 4$ and $\epsilon_{IR} < 0$ when $D > 4$). As U.V. divergent terms cancel each other in the sum mentionned in section 2.3.1, the integral is then U.V. convergent. The I.R. divergent terms remain till the final sum at the level of the cross section, taking into account real photon emission, see section 2.3.2. Once one has achieved the compensation of divergences, one can take the limit $\mathbf{D} \to 4$.

Besides, in order to calculate integrals we use the Feynman parametrization:

$$\frac{1}{A.B} = \int_0^1 \frac{dx}{[xA + (1-x)B]^2} \tag{4}$$

where x is called Feynman parameter. The effect of this parametrization is to reduce by one the number of factors in the denominator.

For example, for the vertex correction diagram, two Feynman parameters will appear as we have three factors in the denominator.

The only integrals which remain to be performed are integrals over Feynman parameters as integrals in **D** dimension over ℓ are given in the literature.

2.4 ***Radiative corrections to virtual Compton scattering***

Virtual Compton scattering is accessible experimentally by p(e,e'p')γ reaction (figure 3).

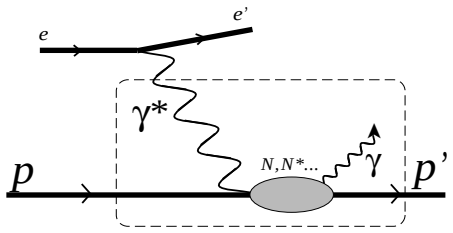

Figure 3: p(e,e'p')γ reaction

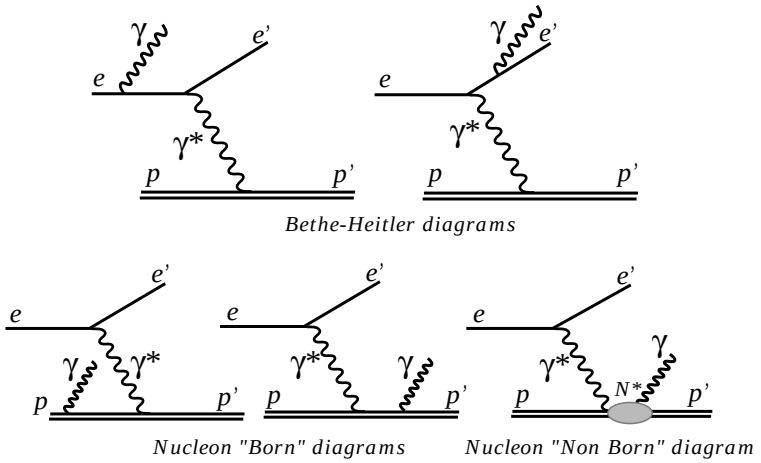

Figure 4: Processes describing the experiment for virtual Compton scattering

In this reaction, the final real photon can be emitted either by the electron or by the proton which is represented on figure 4. The first process is described by Bethe-Heitler amplitude which is calculable from Quantum Electron-Dynamics (QED). The second process is described by the Virtual Compton Scattering (VCS) amplitude, that can be split into two parts: The Born term containing only the nucleon and the anti-nucleon contributions (exactly calculable and determined precisely in reference [3]) and the Non-Born

term related to the excited states and parametrized by the polarizabilities.

The probability $\mathcal{M}^{exp}$ (which is the differential cross section divided by the phase space factor) is therefore a coherent sum of different amplitudes,

$$\mathcal{M}^{exp} = \frac{1}{4}\sum_{spin} |T^{BH} + T^{VCS}|^2 = \frac{1}{4}\sum_{spin} |T^{BH} + T^{Born} + T^{NonBorn}|^2 \quad (5)$$

The low energy theorem from Low[7] says that in an expansion in powers of outgoing photon energy (q') in the final photon-proton centre of mass system, the two first terms of the probability M, of the order q'^{-2} and q'^{-1} are only due to the interference of the B.H. and Born amplitudes and are completely calculable. The effect of polarizabilities appears from the q'^0 term.

At small q', below pion threshold production, the cross section is dominated by the B.H. and the Born contributions. We can calculate exactly the radiative corrections to $|T^{BH} + T^{Born}|^2$ (see subsection 2.3) and assume that the same correction can be applied to the complete cross section.

We will then obtain the corrected cross section in dividing the measured cross section by the radiative correction factor to $|T^{BH} + T^{Born}|^2$:

$$\mathcal{M}^{exp}_{corrected} = \mathcal{M}^{exp}_{measured}/(1 + \delta_v + \delta_r) \quad (6)$$

where δ_v is for virtual radiative correction and δ_r for real radiative correction.

2.5 ***Radiative corrections to*** $|T^{BH} + T^{Born}|^2$

Half of the diagrams which have to be taken into account are represented on figure 5. The missing ones are crossed diagrams.

Self-energy and real photon emission corrections on the proton are expected to be small due to its large mass. They are neglected here, but will be calculated in the future. In addition, the exhange of a second virtual photon between the electron and the proton has been found negligible according to references [8,9].

Bethe-Heitler and Born processes have their cross section proportional to α^3 and we need to take into account higher order terms which contribution to the cross section is in α^4 to determine radiative corrections. On figure 5, we can notice that Bremsstrahlung cross section is in α^4 and that virtual radiative corrections graphs are in $\alpha^2\sqrt{\alpha}$. Thus one can write the corrected cross section as:

$$\mathcal{M}^{BH+Born}_{measured} = |\mathcal{T}^{BH} + \mathcal{T}^{Born}|^2 + 2.\mathcal{R}e(\mathcal{T}^{BH} + \mathcal{T}^{Born})(V.R.C) + |R.R.C|^2 \quad (7)$$

- $V.R.C$: Virtual Radiative Corrections amplitude,

- $R.R.C$: Real Radiative Corrections amplitude.

In reference to (Eq. 2), one can either express the measured cross section as:

$$\mathcal{M}^{BH+Born}_{corrected} = |\mathcal{T}^{BH} + \mathcal{T}^{Born}|^2(1 + \delta_v + \delta_r) \tag{8}$$

For virtual radiative corrections, rather than aiming for an analytical formula, which would have been long and complicated, a crafty "trick" has been used to evaluate I.R. divergent part of integrals appearing in the expression of graphs. As a matter of fact, for each diagram, a specific term that contains the divergence is added and substracted, see reference [9]. The result is that only the added term contains the divergence whereas others terms do not. Therefore, the corresponding integrals of the non divergent part can be performed directly in four dimensions. Besides, one can notice that the divergent part is the same as the one occuring in radiative corrections to elastic scattering and therefore leads to an analytical term after having verified the cancellation of I.R. divergent terms. The finite four dimensional integral is evaluated introducing three Feynman parameters and will be performed numerically.

One can then re-write the equation (8) in the form:

$$\mathcal{M}^{LET}_{measured} = |\mathcal{T}^{BH} + \mathcal{T}^{Born}|^2(1 + \mathcal{P}^{anal}_{R.R.C} + \mathcal{P}^{anal}_{V.R.C} + \mathcal{P}^{num}_{V.R.C}) \tag{9}$$

and we can now express δ_v and δ_r as:

- $\delta_v = \mathcal{P}^{anal}_{V.R.C} + \mathcal{P}^{num}_{V.R.C}$

- $\delta_r = \mathcal{P}^{anal}_{R.R.C}$

δ_r is given by:

$$\delta_r = \frac{e^2}{4\pi^2}\, 2\, \ln\frac{\Delta E}{E}\Big[\frac{v^2+1}{2v}\, \ln\frac{v+1}{v-1} - 1\Big] \tag{10}$$

$v = 1 + \frac{4m^2}{Q^2}$ where Q^2 is the square 4-momentum transfered to the virtual photon and m the electron mass. As one may notices, δ_r is dependent on the cut in energy ΔE and on the energy E of electron.

The experiment is performed by detecting in coincidence the outgoing electron and the proton. The real photon is reconstructed through 4-momentum conservation law. Compton events are then identified by reconstructing the missing mass square. The cut ΔM^2_{miss} is related to ΔE. The figure 6 shows the events corrected for radiative corrections as a function of ΔM^2_{miss}. For

$\Delta M^2_{miss} > 500 MeV^2$ we can see that the curve reaches a plateau which means that, above this cut, the experimental resolution does not affect the cross section. Besides, the correction applied is well compensating radiative events eliminated by the experimental cut. On figure 7, for $q' = 45 MeV$ this correction is about 18% when $\Delta M^2_{miss} = 1000 MeV^2$, $\Delta E = 15 MeV$.

The numerical evaluation of $\mathcal{P}^{num}_{V.R.C}$, found in Eq. (9) is a challenging numerical problem as the only mass scales in the calculation are the electron mass and its energy. Due to the large ratio between them, the Feynman parameter integrals contain integrable singularities in very narrow regions of Feynman parameter space for which we have developped specialized integration routines. Most diagrams are already calculated and we are about to finishing the calculation of the remaining ones.

Therefore, radiative corrections made on data and presented on figure 7 as a **PRELIMINARY RESULT** are evaluated without the contribution of the numerical term, $\mathcal{P}^{num}_{V.R.C}$ but do contain the analytical part $\mathcal{P}^{anal}_{V.R.C}$.

2.6 ***Conclusions***

On figure 7, we can see that the partially corrected data points are close to the theoretical predicted cross section $|T^{BH} + T^{Born}|^2$.

As for this energy of q'=45MeV we expect very small polarizabilities effect, the full corrected measurements are expected to be in agreement to the above prediction. Therefore a preliminary conclusion could be that the missing numerical part of the correction should be very small.

The final results will answer this question for this q'=45MeV kinematics, and also for all other kinematics performed experimentally.

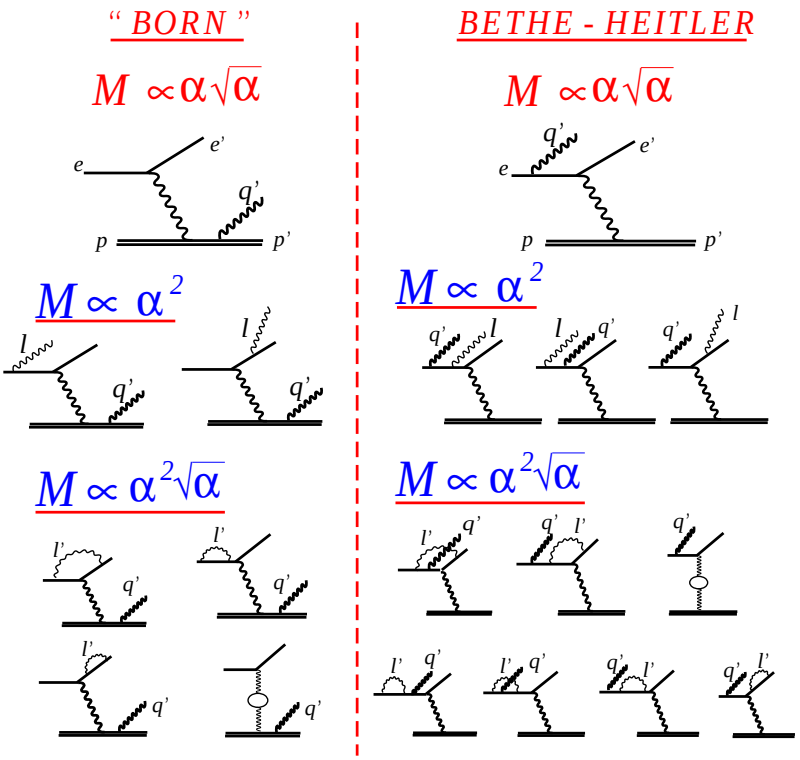

Figure 5: Born, Bethe-Heitler and first order radiative corrections diagrams to VCS. This figure represents only one half of the graphs which have to be taken into account as we have to consider crossed diagrams. $\mathbf{l}, \mathbf{l}'$ are respectively the energy of the soft photon emitted and the 4-momentum of the virtual photon. $\mathbf{q}'$ is the energy of the real final photon. $\mathcal{M}$ is the scattering amplitude and α the fine-structure constant.

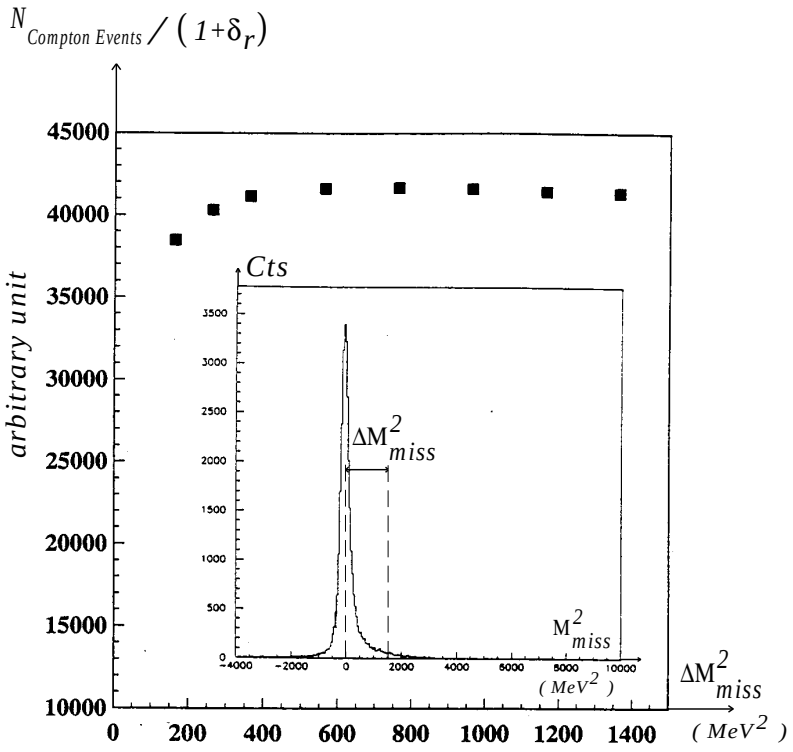

Figure 6: The central part of the figure represents Compton events as a function of M^2_{miss} and we can notice the radiative tail on the right side of the peak. The main plot corresponds to Compton events as a function of ΔM^2_{miss}. Note that for $\Delta M^2_{miss} > 500 MeV^2$, this function is independent of the cut. If we take $\Delta M^2_{miss} = 1000 MeV^2$, $\Delta E = 15 MeV$, the real radiative correction is about 18% in the kinematics of q'=45MeV

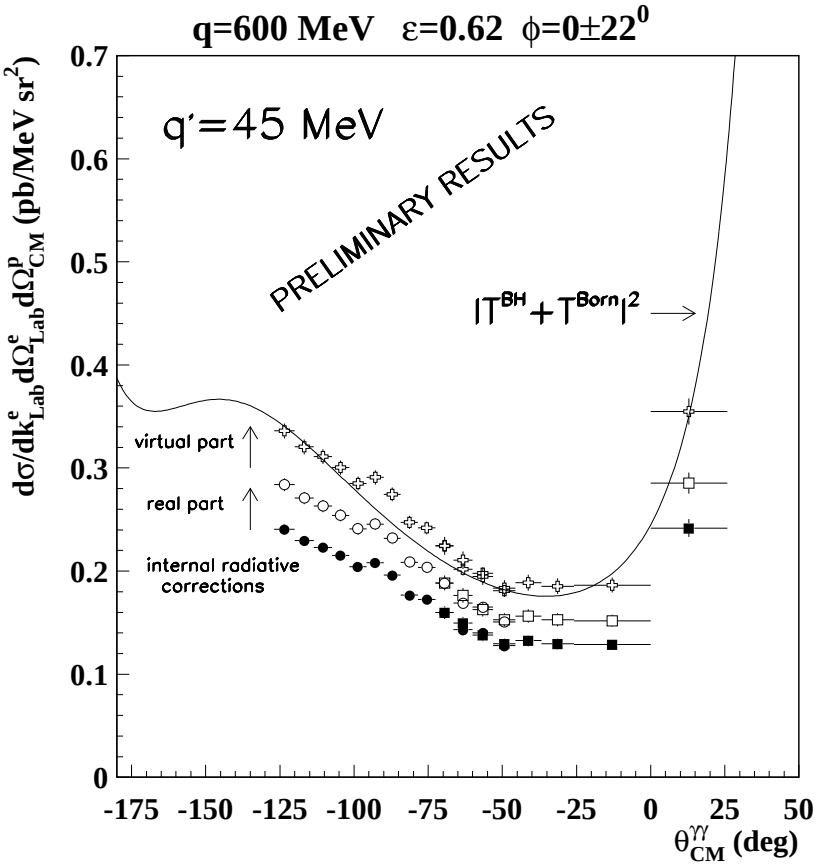

Figure 7: Preliminary differential cross sections at q'=45MeV. The two sets of solid points (circles and squares) are experimental data corrected for external radiative corrections. They are obtained with two different settings of the proton spectrometer. We can note that data in the overlapping region (around 60°) are in good agreement. The blank circles and squares correspond to data corrected for real radiative corrections. The blank crosses are data corrected for almost total internal radiative corrections: real and virtual contributions. For now, only the analytical term of virtual radiative corrections is taken into account , the numerical term remains to be computed. The solid line represents the differential cross section with only B.H. and Born contributions. At q' as small as 45MeV, we expect a good agreement between the data and this theoretical cross section as it is the first test of the low energy theorem for VCS.

References

1. J. Roche: Contribution to the proceedings.
2. L. Van Hoorebeke: Contribution to the proceedings.
3. P.A.M. Guichon, G. Liu, A.W. Thomas, Nucl. Phys. **A591** (1995).
4. F. Bloch and A. Nordsiek, Phys. Rev. 52 (1937).
5. C. de Calan, H. Navelet, J. Picard, Note CEA-N-2624.
6. G. Leibbrandt, Rev. Mod. Phys. 47 (1975).
7. F.E. Low, Phys. Rev. 96 (1954) 1428.
8. E. Amaldi, S. Fubini, G. Furlan, Pion-Electroproduction, Springer Tracts in Mod. Physics (1983).
9. L.W. Mo, Y.S. Tsai, Rev.of Mod. Phys. 41 (1969) 205.
10. M. Vanderhaeghen et al., in preparation.